High-pressure structural studies of dysprosium using angle-dispersive x-ray diffraction

Yong Rong Shen,* Ravhi S. Kumar,† Andrew L. Cornelius, and Malcolm F. Nicol
Department of Physics and High Pressure Science and Engineering Center, University of Nevada Las Vegas, Las Vegas, Nevada 89154-4002, USA

(Received 28 April 2006; revised manuscript received 16 November 2006; published 28 February 2007)

We present structural results under pressure for elemental dysprosium (Dy) up to 87 GPa using *in situ* angle-dispersive x-ray diffraction measurements with synchrotron x rays and a diamond-anvil cell. Dy exhibits the structural transition sequence, hP2 → hR9 → hP4 → distorted cF4, from Rietveld full-profile refinements. Clear evidence is documented for the high-pressure distorted cF4 phase observed above 45 GPa to be an orthorhombic oS8 (*Cmmm*) structure for Dy in the lanthanide phase diagram.

DOI: 10.1103/PhysRevB.75.064109 PACS number(s): 81.40.Vw, 61.10.Eq

I. INTRODUCTION

The high-pressure behavior of elemental lanthanides continues to attract considerable interest in understanding fundamentals in the lanthanide series, such as structural stability, systematics at high pressures and temperatures, and 4*f* delocalization and its role in the structures induced by pressure and temperature[1–3] The lanthanide elements Tb and Dy, which are isostructural at ambient conditions, exhibit similar phase transition sequences, hP2 → hR9 → hP4 → distorted cF4 (Pearson's notation), on increasing pressure.[4–6] Compression leads to 4*f* delocalization, and low-symmetry structures are observed at high pressures in almost all lanthanide elements in this series, such as Ce, Pr, Sm, and Nd.[7–14] In general, the origin of such low-symmetry phases is due to the delocalized 4*f* electrons participating in the metallic bonding. It is also interesting that the high pressure phases of 4*f* elements resemble the structures exhibited by the 5*f* elements, indicating similarity of *f* electrons in both lanthanides and light actinide elements. Even though experiments on the *f*-electron behavior and phase transitions under pressure are available, a definite structural assignment for the high-pressure dcF4 phase in the phase transition sequence has not yet been reported. This is due to the lack of high-resolution powder-diffraction data at extreme pressures. Dy, which crystallizes in the hP2 structure at ambient conditions, is an ideal candidate for the study of the post-cF4 phases due to the 4*f* delocalization. It may also serve as a structural model for neighboring lanthanide elements under pressure. Hence, the present work aimed to study the high-pressure phases of Dy in detail and to attempt a successful structural assignment for the long debated distorted cF4 phase. In order to cover the whole phase transition range, we performed high-resolution angular-dispersive x-ray powder-diffraction experiments with an imaging plate and diamond-anvil cell pressures up to 87 GPa. We discuss our diffraction results, with full profile Rietveld structural refinements for the post-cF4 phase above 45 GPa with a number of possible high pressures and present evidence for an orthorhombic oS8 (*Cmmm*) assignment for the dcF4 phase of Dy which persists at least up to 87 GPa.

II. EXPERIMENTAL DETAILS

Dysprosium metal provided commercially by American Elements with a stated purity of 99.99% was used to perform high-pressure x-ray-diffraction measurements at the 16ID-B undulator beam line by the high pressure collaborative access team (HPCAT) at the Advanced Photon Source (APS). A double crystal branching monochromator consisting of water-cooled diamond (111) and silicon (220) crystals provided a monochromatic x-ray beam with a wavelength of 0.4218 Å. The resolution of the monochromator is about $\Delta\lambda/\lambda = 10^{-3}$. The monochromatic x-ray beam was focused down to a size of $30 \times 30\ \mu m^2$ using multilayer bimorph mirrors in a Kirkpatrick-Baez configuration, and the focused beam approached the sample through a 30 μm pinhole. Diffraction patterns were acquired with an image plate detector (MarCCD 345) using an exposure time of 10 s. The distance between the sample and the detector and the inclination angle of the image plate were calibrated using a CeO_2 standard. The high-resolution image plate angle-dispersive x-ray-

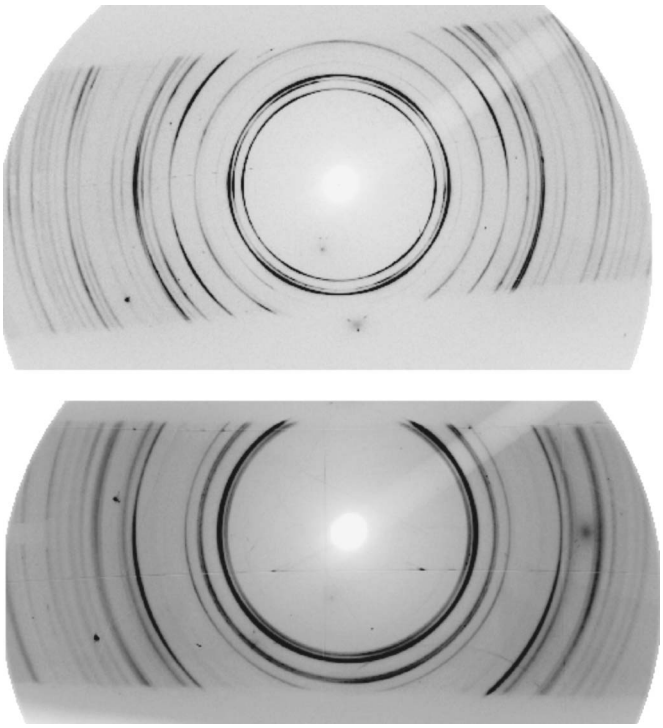

FIG. 1. X-ray-diffraction images of Dy at 4.2 GPa (top) and 87 GPa (bottom) at room temperature (10 s exposure time and $\lambda = 0.4218$ Å).

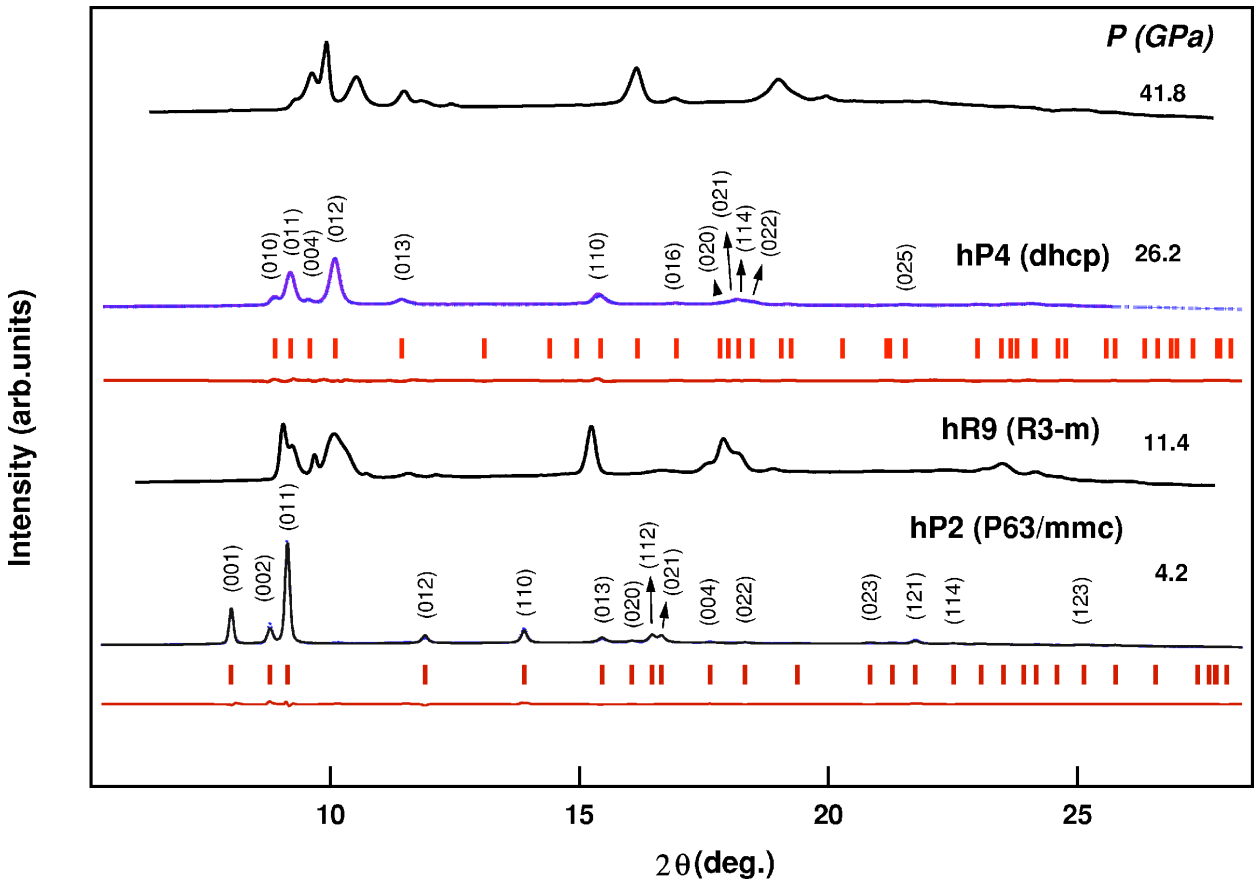

FIG. 2. (Color online) Representative high-pressure diffraction patterns of Dy at room temperature showing the phase transitions with the data for Rietveld full-profile refinement incorporated for hP2 and hP4 phases.

diffraction technique at the HPCAT ID-B beamline allowed us to obtain high-quality Debye-Scherrer ring patterns. For instance, Fig. 1 displays the x-ray-diffraction pattern images of Dy at 4.2 and 87 GPa.

For our data analysis, two-dimensional images were first integrated to one dimensional intensities (counts) as a function of diffraction angle (2θ) using the FIT2D software.[15] The GSAS and LHPM-RIETICA packages were successfully used to perform Rietveld structural refinements for the diffraction data over the entire pressure range up to 87 GPa.[16,17] Preferred orientation was taken into account for Rietveld full-profile structural refinements over the entire pressure range between ambient pressure and 87 GPa, and was observed to be small and to remain almost constant with pressure. Texture is also considered while processing the diffraction images through FIT2D, and on increasing pressure, the patterns were found to be less affected.

High pressures were generated by a Mao-Bell-type diamond-anvil cell (DAC). A 130 μm sample chamber was formed in a rhenium metal gasket with a preindention of 60 μm thickness. In order to avoid oxidization of the Dy sample, exposure to air was minimized by loading the sample immersed in the silicone fluid pressure media.[18] For pressure determination, the standard ruby fluorescence technique[19] was employed, and the proposed ruby pressure scale form of Holzapfel[20] was used to compute the pressures.

III. RESULTS

Representative diffraction spectra of elemental Dy at several pressures between ambient and 45 GPa are shown in Fig. 2. The initial structure of the elemental Dy was a regular hexagonal-close-packed form (hP2, $P6_3/mmc$). This form is found in heavier lanthanide metals over the entire second half of the lanthanide series at ambient conditions.[1] Upon compression, the hP2 form of Dy began to transform to the Sm-type structure (hR9, $R\bar{3}m$) around 7 GPa. The cell parameters of hR9 at 7 GPa are $a=3.4014(7)$ Å and $c=24.56(2)$ Å. This hP2$\rightarrow$hR9 phase transformation was observed to be very sluggish and took place until the pressure induces a second structural transformation from hR9 to a regular double hexagonal-close-packed phase (hP4, $P6_3/mmc$) at about 17 GPa. In contrast, Dy underwent an hR9$\rightarrow$hP4 phase transformation and, above 19 GPa, a pure hP4 phase. The cell parameters at 18.8 GPa are $a=3.2217(5)$ Å and $c=10.3460(4)$ Å. As pressure is raised further to about 39 GPa, we observed a face-centered-cubic phase (cF4, $Fm\bar{3}m$) coexisting with the hP4 phase. Table I summarizes the observed and calculated d values for hP2 and hR9 phases.

Upon further compression, the so-called distorted face-centered-cubic structure (d-cF4) persisted up to a maximal pressure of 87 GPa, beginning from 43 GPa. Figure 4 repre-

TABLE I. Observed 2θ values, corresponding d values (d_0), calculated d values (d_c), intensities, and (hkl) values are listed for hP2 and hR9 structures.

P=4.2 GPa hP2 ($P63/mmc$) a=3.4936(7) Å b=5.506(2) Å						P=7 GPa hR9 ($R\bar{3}m$) a=3.4014(7) Å c=24.56(2) Å					
2θ (deg)	(hkl)	d_0 (Å)	d_c (Å)	σd	I/I_0 (%)	2θ (deg)	(hkl)	d_0 (Å)	d_c (Å)	σd	I/I_0 (%)
8.001	(100)	3.0231	3.0256	0.0025	95	8.271	(101)	2.9244	2.9247	0.004	65
8.775	(002)	2.7568	2.7532	0.0036	65	8.445	(012)	2.8643	2.8644	0.0002	25
9.130	(101)	2.6497	2.6517	0.0020	100	8.866	(009)	2.7285	2.7289	0.0004	100
11.892	(102)	2.0359	2.0363	0.0005	8.2	9.116	(104)	2.6538	2.6559	0.0021	26
13.865	(110)	1.7474	1.7468	0.0005	62	9.578	(015)	2.5261	2.5263	0.0002	82
15.441	(103)	1.5699	1.5693	0.0006	10	14.245	(110)	1.009	1.7007	0.0002	69
16.036	(200)	1.5120	1.5128	0.0008	8.4	16.503	(021)	1.4695	1.4702	0.0007	8.4
16.452	(112)	1.4740	1.4750	0.0010	28	16.578	(202)	1.4629	1.4624	0.0005	15.3
16.626	(201)	1.4587	1.4587	0.0000	28	16.813	(119)	1.4426	1.4433	0.0003	48.4
17.597	(004)	1.3788	1.3766	0.0022	5	16.935	(024)	1.4323	1.4322	0.0001	19.9
18.307	(202)	1.3257	1.3258	0.0001	3	17.199	(205)	1.4104	1.4108	0.0004	13.6
19.378	(104)	1.2531	1.2530	0.0001	1	17.783	(00 18)	1.3645	1.3644	0.0001	4.7
20.824	(203)	1.1670	1.1674	0.0004	5	17.820	(10 16)	1.3616	1.3613	0.0003	6.8
21.214	(210)	1.1441	1.1436	0.0006	6	17.871	(027)	1.3578	1.3580	0.0002	6.8
21.707	(211)	1.1200	1.197	0.0004	22	20.925	(02 13)	1.1614	1.1616	0.0002	2.1
22.482	(114)	1.0819	1.0812	0.0007	2.6	21.857	(211)	1.1124	1.1122	0.0002	6.8
23.046	(212)	1.0558	1.0561	0.0003	2.4	21.924	(122)	1.1091	1.1088	0.0003	8.7
23.550	(105)	1.0355	1.0349	0.0014	2.3	22.187	(214)	1.0961	1.0955	0.0006	17.2
24.132	(300)	1.0089	1.0085	0.0004	4	22.395	(125)	1.0861	1.0858	0.0003	11
25.114	(213)	0.9701	0.9706	0.0005	2.8	22.859	(11 18)	1.0643	1.0645	0.0002	4.7
25.743	(302)	0.9467	0.9470	0.0003	2.2	22.894	(02 16)	1.0627	1.0628	0.0001	4.7
						22.926	(217)	1.0612	1.0614	0.0002	4.6
						23.597	(20 17)	1.0314	1.0315	0.0001	2.6
						23.787	(00 24)	1.0233	1.0234	0.0001	2.5
						24.010	(21 10)	1.0139	1.0138	0.0001	2.4
						24.807	(300)	0.9819	0.9821	0.0003	3.1

sents some typical x-ray-diffraction spectra for the distorted cF4 (d-cF4) phase of Dy between 46.1 and 87 GPa. From Figs. 3 and 4, we can clearly see that the hP4 (dhcp) underwent a structural change to the d-cF4 phase above 42 GPa.

Diffraction peaks in the 87 GPa spectrum, specifically labeled L1, L2, and L3 in Fig. 3, exhibited a clear doublet feature in peak L1 and splitting in peaks L2 and L3. These features were found to begin from 46.1 GPa. We have pro-

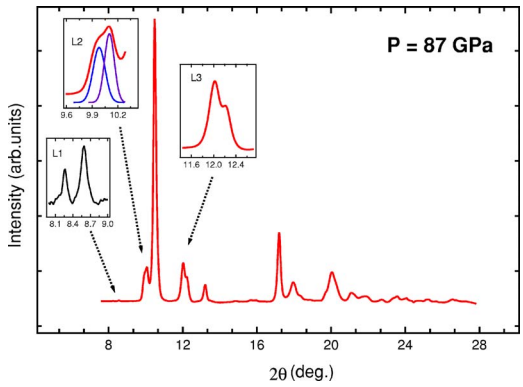

FIG. 3. (Color online) Diffraction pattern of Dy at 87 GPa. The peaks labeled L1, L2, and L3 as insets are zoomed to show the doublet features in the spectrum.

vided the observed and calculated d values for the hP4 and oS8 phases of Dy in Table II, which will be discussed further in the next section.

IV. DISCUSSION

Upon compression, the regular trivalent lanthanides exhibit a sequence of phase transitions to simple polytypical close-packed structures (hcp→Sm type→dhcp→fcc or hP2→hR9→hP4→cF4) before undergoing further transitions to the so-called distorted face-centered-cubic (using d-fcc or d-cF4) phase and then to more complicated higher pressure phases, such as the Sm-V, α''-Ce, and α-U structures.[21] It is well known that pressure induces the low-symmetry d-cF4 phase from an ideal cF4 structure in a subtle and continuous manner. There have been many structural models for this d-cF4 phase, but a definite and unique structural identification has not yet been made.

Several earlier structural models had assigned the d-cF4 phase as a triple hexagonal-close-packed structure ($P6_3/mmc$ or $P\bar{6}m2$),[22–24] a trigonal structure ($P3_221$),[25] an orthorhombic structure with 16 atoms per unit cell,[26] or a monoclinic structure ($P2_1/m$ or $P2_1/c$).[27] In 1993, Hamaya *et al.*[28] studied high-pressure synchrotron x-ray diffractions on elemental praseodymium and proposed an assignment of another trigonal structure ($R\bar{3}m$, hR24) to the d-cF4 phase. Later, another monoclinic structure ($C2/m$) with four atoms per unit cell was proposed as the d-cF4 in the high-pressure x-ray-diffraction studies on Ce and Pr.[29,30] Recently Patterson *et al.*[31] studied Dy and reported a simple monoclinic bcm phase above 73.3 GPa. They adopted the atomic positions suggested by Hamaya *et al.*, with an hR24 structure, to 69.4 GPa, and a 6% volume collapse has been reported during the bcm transition.

It has been more commonly accepted that cF4→d-cF4 structural transformation because of a slight structural distortion should be a continuous (or nearly continuous) second-

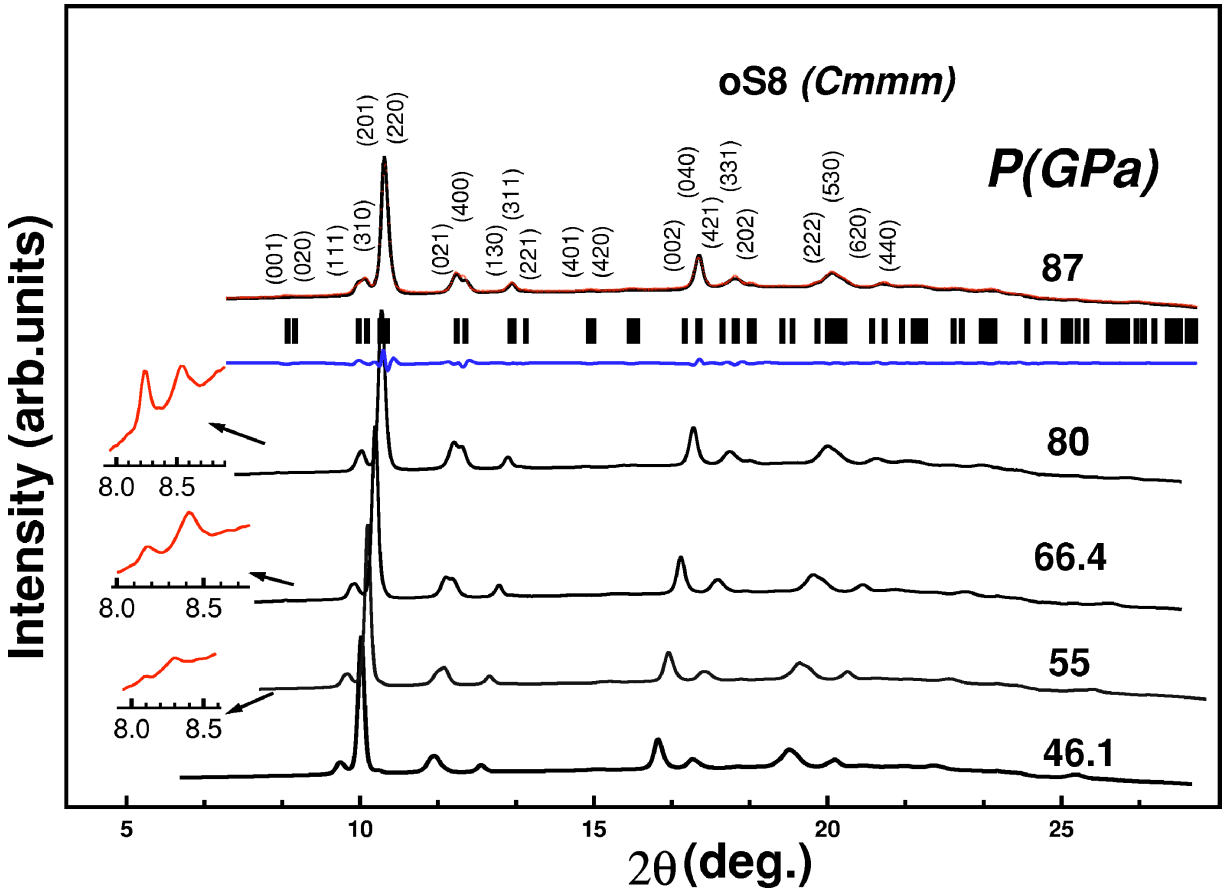

FIG. 4. (Color online) X-ray-diffraction patterns collected at various pressures from 46.1 to 87 GPa.

TABLE II. Observed 2θ values, corresponding d values (d_0), calculated d values (d_c), intensities, and (hkl) values are listed for hP4 and oS8 structures.

P=26.2 GPa hP4 ($P63/mmc$) a=3.145(1) Å b=10.117(2) Å						P=87 GPa oS8 ($Cmmm$) a=7.8958(7) Å, b=5.6307(1) Å c=2.922(1) Å					
2θ (deg)	(hkl)	d_0 (Å)	d_c (Å)	σd	I/I_0 (%)	2θ (deg)	(hkl)	d_0 (Å)	d_c (Å)	σd	I/I_0 (%)
8.888	(100)	2.7225	2.7242	0.0016	25	8.254	(001)	2.9301	2.9225	0.0076	0.4
9.203	(101)	2.6288	2.6305	0.0007	72	8.592	(020)	2.8252	2.8154	0.0001	0.6
9.562	(004)	2.5305	2.5298	0.0005	11	9.887	(111)	2.4474	2.4540	0.0066	10
10.10	(102)	2.3958	2.3960	0.0002	100	10.156	(310)	2.3827	2.3843	0.0016	12
11.450	(103)	2.1142	2.1149	0.0007	15	10.290	(201)	2.3518	2.3487	0.0032	11
13.084	(104)	1.8511	1.8519	0.0008	2	10.560	(220)	2.2919	2.2922	0.0004	100
14.952	(105)	1.6209	1.6215	0.0006	4	11.934	(021)	2.0287	2.0274	0.0013	13.7
15.387	(110)	1.5753	1.5748	0.0005	58	12.253	(400)	1.9762	1.9740	0.0022	8.8
16.938	(106)	1.4320	1.4338	0.0018	4.4	13.106	(311)	1.8480	1.8473	0.0006	3
17.839	(200)	1.3602	1.3609	0.0007	11	13.257	(130)	1.8270	1.8260	0.0010	6.2
18.168	(114)	1.3358	1.3356	0.0002	31	13.425	(221)	1.8044	1.8035	0.0009	1.6
18.472	(202)	1.3140	1.3148	0.0008	22	14.807	(401)	1.6367	1.6357	0.0010	0.3
19.202	(008)	1.2645	1.2646	0.0001	5	14.980	(420)	1.6179	1.6163	0.0017	0.3
21.511	(205)	1.1301	1.1304	0.0003	2.7	15.655	(131)	1.5486	1.5485	0.0010	0.5
23.631	(210)	1.0300	1.0296	0.0003	5	15.871	(330)	1.5276	1.5281	0.0005	0.5
24.058	(00 10)	1.0120	1.0117	0.0003	10.6	15.957	(510)	1.5194	1.5205	0.0011	0.5
24.730	(213)	0.9849	0.9848	0.0001	2.2	17.148	(421)	1.4146	1.4143	0.0003	11
26.853	(300)	0.9083	0.9083	0.0002	1.2	17.225	(040)	1.4084	1.4077	0.0007	24.5
						17.392	(112)	1.3950	1.3920	0.0029	8.7
						17.906	(331)	1.3552	1.3541	0.0011	5.1
						17.991	(511)	1.3489	1.3488	0.0001	6.5
						18.308	(240)	1.3257	1.3259	0.0002	2.4
						18.449	(600)	1.3156	1.3160	0.0004	1.9
						19.671	(222)	1.2346	1.2320	0.0026	3
						20.119	(241)	1.2079	1.2074	0.0005	10
						20.231	(601)	1.2008	1.1999	0.0009	7.8
						20.383	(620)	1.1919	1.1922	0.0003	5.4
						21.203	(440)	1.1463	1.1461	0.0002	2.7
						21.285	(132)	1.1420	1.1408	0.0012	2.3

TABLE II. (*Continued.*)

$P=26.2$ GPa hP4 ($P63/mmc$) $a=3.145(1)$ Å $b=10.117(2)$ Å						$P=87$ GPa oS8 ($Cmmm$) $a=7.8958(7)$ Å, $b=5.6307(1)$ Å $c=2.922(1)$ Å					
2θ (deg)	(hkl)	d_0 (Å)	d_c (Å)	σd	I/I_0 (%)	2θ (deg)	(hkl)	d_0 (Å)	d_c (Å)	σd	I/I_0 (%)
						21.761	(531)	1.1173	1.1166	0.0007	1.8
						21.810	(150)	1.1148	1.1149	0.0001	2
						21.984	(710)	1.1061	1.1060	0.0001	1.5
						22.028	(621)	1.1039	1.1038	0.0001	1.1
						22.771	(441)	1.0683	1.0670	0.0013	0.9
						23.367	(151)	1.0414	1.0416	0.0002	2.5
						23.507	(350)	1.0352	1.0353	0.0001	2.9
						23.526	(711)	1.0345	1.0344	0.0001	3
						23.989	(042)	1.0148	1.0137	0.0011	1.7

order phase transition. Continuous second-order phase transitions can be predicted by the Landau theory and Lifshitz criteria, based on which, a complete table for all the possible phase symmetries derived from a regular prototypical cF4 phase ($Fm\bar{3}m$) was established by Ben Ghozlen and Mlik[32] in 1983 and by Stokes and Hatch in 1984.[33] Experimental results have further shown that the cF4→d-cF4 structural transformation is essentially due to phonon softening at the L point of the fcc Brillouin zone.[34] Porsch and Holzapfel,[35] in 1994, and Seipel *et al.*,[36] in 1997, carefully inspected all possible continuous and discontinuous transitions for the d-cF4 phase induced by pressure in the entire lanthanide series and found only few structural candidates with one single-component order parameter for the d-cF4 phase, two orthorhombic structures [*Cmmm* (oS8) and *Cmma* (oS8′)], one trigonal structure [$R\bar{3}m$(hR24)], and one triclinic structure ($P\bar{1}$). Among these structures, they proposed that only the *Cmmm* structure can have a continuous transition based on the symmetry arguments.

In order for us to be able to uniquely identify the structure of the d-cF4 phase induced by pressure between 45 and 87 GPa (Fig. 4), we have taken care during data collection to avoid possible interference of the gasket peaks. The gasket hole inspected at every pressure point stayed intact up to the highest pressure achieved in the experiment, yielding high-

TABLE III. Details for five different structures. δ represents the order parameter as a measure of distortions from the regular cF4 structure. The subscripts c, m, o, and h used for cell parameters denote cubic, monoclinic, orthorhombic, and hexagonal lattices, repectively.

Space group	Atomic positions	Cell parameters
$Fm\bar{3}m$ (cF4)	$4a$ (0, 0, 0)	a_c
$C2/m$ (mC4)	$4i$ $(x,0,z)$, $x\approx 1/4+\delta$, $z\approx 1/4-\delta$	$a_m=c_m\approx\sqrt{3/2}a_c$, $b_m\approx(\sqrt{2}/2)a_c$, $\beta\approx\cos^{-1}(1/3)$
Cmma (oS8′)	$4a$ $(1/4,0,0)$, $4g$ $(0,1/4,z)$, $z\approx 1/2+\delta$	$a_o\approx 2a_c$, $b_o\approx\sqrt{2}a_c$, $c_o\approx(\sqrt{2}/2)a_c$
$R\bar{3}m$ (hR24)	$6c$ $(0,0,z')$, $18h$ $(x,-x,z)$, $x\approx 1/2+\delta$, $z\approx 1/4-\delta$, $z'\approx 1/4+3\delta$	$a_h\approx\sqrt{2}a_c$, $c_h\approx 2\sqrt{3}a_c$
Cmmm (oS8)	$4g$ $(x,0,0)$, $4j$ $(0,y,1/2)$, $x\approx 1/4+\sqrt{2}\delta$, $y\approx 1/4+\delta$	$a_o\approx 2a_c$, $b_o\approx\sqrt{2}a_c$, $c_o\approx(\sqrt{2}/2)a_c$

TABLE IV. Cell and atomic position parameters for the x-ray-diffraction pattern of Dy at 87 GPa and at room temperature.

Space group	Atomic position parameters	Cell parameters (Å)	Refinement residual (*wRp*) (%)
$Fm\bar{3}m$ (cF4)		a_c=3.9778(1)	13.7
$C2/m$ (mC4)	x=0.3154(3), z=0.2539(2)	a_m=4.8597(1), b_m=2.8180(1), c_m=4.8431(1), β=108.43(20)°	7.4
Cmma (oS8′)	z=0.6420(2)	a_o=7.8723(1), b_o=5.6398(1), c_o=2.8420(1)	7.7
$R\bar{3}m$ (hR24)	x=0.50399(1), z=0.2645(2), z'=0.3017(2)	a_t=5.6256(1), c_t=13.767(2)	8.3
Cmmm (oS8)	x=0.2121(1), y=0.2677(1)	a_o=7.8958(1), b_o=5.6307(1), c_o=2.922(1)	6.7

quality diffraction spectra. The splitting observed between 2θ=8° and 9°, as discussed previously, were shown as an inset in Fig. 3 at 87 GPa and in Fig. 4 above 40 GPa.

We have attempted to use structural models proposed in the literature and often used for the d-cF4 phase in prior high-pressure structural studies in elemental lanthanides (Table III). We began by using a regular cF4 structure to perform a Rietveld full-profile refinement. This procedure allowed us to differentiate cF4 parental peaks and superlattice peaks due to the distortion, and also provided initial values for cell parameters of a proposed structure given in Table III. Their values are used for structural refinement.

Table IV and Fig. 5 summarize our results for Rietveld refinements on Dy at 87 GPa. First, note that the monoclinic structure (mC4) cannot predict the observed doublet feature in peak L1 (Fig. 3). The cell parameters provided in Ref. 31 for the possible bcm phase also did not yield any good fits. From this, the possibility of a monoclinic bcm high-pressure phase can be excluded. Second, note that the trigonal structure (hR24) cannot predict the observed doublet feature in peak L1 and the observed splitting in peaks L2 and L3. As a result, it can also be excluded. Third, the orthorhombic structure [*Cmma* (oS8′)] should be excised from the proposed structural models because it is unable to predict the splitting in peak L2. We have also considered the triclinic P1 space group for our fitting, but the simulated pattern requires at least three lower angle peaks in addition to the observed doublet. Moreover, the refinement residual is found to be higher than the orthorhombic *Cmmm* phase. Finally, the remaining structural model, which is the orthorhombic structure [*Cmmm* (oS8)], satisfied the requirement of continuous second-order phase transitions, yielding an excellent agreement between the model calculation and the experiment.

Rietveld full-profile refinements of angle-dispersive synchrotron x-ray-diffraction data for dysprosium with five phases over the entire pressure range were made and pro-

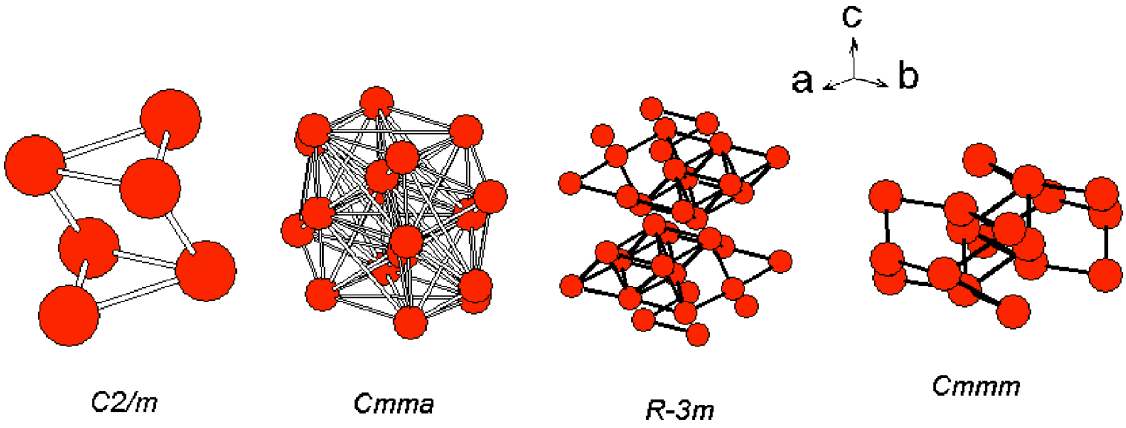

FIG. 5. (Color online) Various structural models considered in Table IV for the dcF4 phase of Dy.

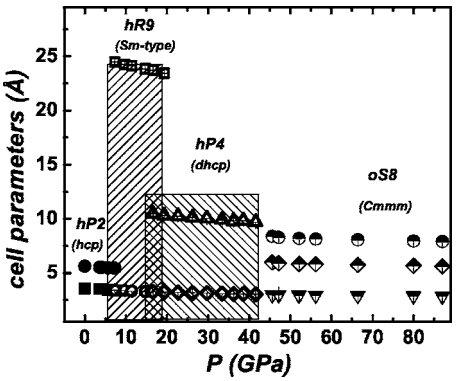

FIG. 6. Cell parameters for various high-pressure phases obtained through the refinements performed for Dy.

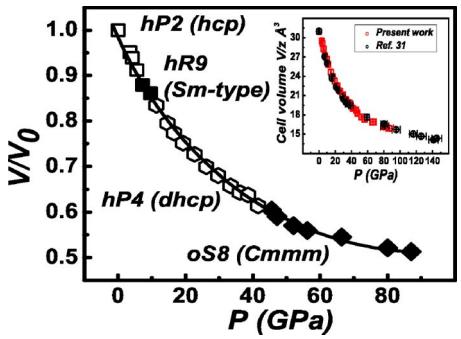

FIG. 7. (Color online) Pressure-volume data fitted with the Birch-Murnaghan equation of state. The inset shows the volume as a function of pressure compared with the shock wave data (Ref. 39).

duced cell parameters and cell volumes as functions of pressure (Fig. 6). The bulk modulus is calculated by fitting the pressure-volume data of Dy using the Birch-Murnaghan equation[37]

$$P = 3/2B_0[(V_0/V)^{7/3} - (V_0/V)^{5/3}] \times\left\{1 + \tfrac{3}{4}(B_0' - 4)[(V_0/V)^{2/3} - 1]\right\},$$

where V_0 is the volume at ambient conditions, B_0 is the average bulk modulus, and B_0' is the first derivative of the bulk modulus. The equation of state is shown in Fig. 7. The fit yielded a bulk modulus value $B_0 = 36.3 \pm 2$ GPa and a pressure derivative $B_0' = 3.71 \pm 0.14$. The average bulk modulus value for Dy reported by Grosshans and Holzapfel[38] is 40 GPa with $B_0' = 2.9$; the bulk modulus value obtained in our present study compares well with the shock data[39] and with the static experimental results (bcm transition) reported in Ref. 31 for Dy.

In summary, we have studied elemental Dy to pressures up to 87 GPa and have presented the structural parameters using the Rietveld full profile refinement. The post-cF4 phase above 45 GPa is clearly assigned to an orthorhombic oS8 (*Cmmm*) structure. Our experimental results warrant further theoretical calculations to ascertain the phase transition under pressure.

ACKNOWLEDGMENTS

We gratefully acknowledge the use of the HPCAT facility supported by DOE-BES, DOE-NNSA, NSF, DODTACOM, and the W. M. Keck Foundation. HPCAT is a high pressure collaborative access team among the Carnegie Institution, The Lawrence Livermore National Laboratory, the University of Hawaii, the University of Nevada Las Vegas, and the Carnegie/DOE Alliance Center. We thank Maddury Somarazulu and the other HPCAT staff for technical assistance and we also thank Wilfred B. Holzapfel for fruitful discussions. This research was supported by the U.S. Department of Energy Cooperative (Agreement No. DE-FC52-01NV14049 with the University of Nevada Las Vegas.

*Deceased.
†Electronic address: ravhi@physics.unlv.edu

[1] U. Benedict, in *Handbook on the Physics and Chemistry of the Actinides*, edited by A. J. Freeman and G. H. Lander (Elsevier Science, Amsterdam, 1987), Vol. 5, Chap. 3, p. 227.
[2] U. Benedict and W. B. Holzapfel, in *Handbook on the Physics and Chemistry of the Rare Earths*, edited by K. A. Gschneider, Jr., L. Eyring, G. H. Lander, and G. R. Choppin (Elsevier Science, Amsterdam, 1993), Vol. 17, Chap. 113, p. 245.
[3] U. Bendeict, J. Alloys Compd. **223**, 216 (1995).
[4] Y. C. Zhao, F. Porsch, and W. B. Holzapfel, Phys. Rev. B **50**, 6603 (1994).
[5] W. B. Holzapfel, J. Alloys Compd. **223**, 170 (1995).
[6] M. G. Pravica, E. Romano, and Z. Quine, Phys. Rev. B **72**, 214122 (2005).
[7] B. Johansson, Philos. Mag. **30**, 469 (1974).
[8] S. Gordon, J. Appl. Phys. **53**, 9212 (1982).
[9] J. R. Peterson, U. Benedict, C. Dufour, I. Birkel, and R. G. Haire, J. Less-Common Met. **93**, 353 (1983).
[10] Y. C. Zhao, F. Porsch, and W. B. Holzapfel, Phys. Rev. B **52**, 134 (1995).
[11] M. I. McMahon and R. J. Nelmes, Phys. Rev. Lett. **78**, 3884 (1997).
[12] Y. K. Vohra, S. L. Beaver, J. Akella, C. A. Ruddle, and S. T. Weir, J. Appl. Phys. **85**, 2451 (1999).
[13] J. Akella, S. T. Weir, Y. K. Vohra, H. Prokop, S. A. Catledge, and G. N. Chesnut, J. Phys. C **11**, 6515 (1999).
[14] G. N. Chesnut and Y. K. Vohra, Phys. Rev. B **62**, 2965 (2000).
[15] A. P. Hammersley, S. O. Svensson, M. Hanfland, A. N. Fitch, and D. Hausermann, High Press. Res. **14**, 235 (1996).
[16] A. C. Larson and R. V. von Dreele, *GSAS Technical Manual* (Los Alamos National Laboratory, Los Alamos, 1985).
[17] J. Howard and B. A. Hunter, A Computer Programme for Reitveld Analysis of X-ray and Neutron Powder Diffraction Patterns, Lucas Height Research Laboratories, 1998.
[18] Y. R. Shen, R. S. Kumar, M. Pravica, and M. F. Nicol, Rev. Sci. Instrum. **75**, 4450 (2004).
[19] R. A. Forman, G. J. Piermarini, J. D. Barnett, and S. Block, Sci-

ence **176**, 284 (1972).
[20] W. B. Holzapfel, J. Appl. Phys. **93**, 1813 (2003).
[21] G. N. Chesnut and Y. K. Vohra, Phys. Rev. B **61**, R3768 (2000).
[22] A. K. McMahan and D. A. Young, Phys. Lett. **105A**, 129 (1984).
[23] G. S. Smith and J. Akella, Phys. Lett. **105A**, 132 (1984).
[24] G. S. Smith and J. Akella, Phys. Lett. **118A**, 136 (1986).
[25] Y. K. Vohra, V. Vijayakumar, B. K. Godwal, and S. K. Sikka, Phys. Rev. B **30**, 6205 (1984).
[26] H. K. Mao, R. M. Hazen, P. M. Bell, and J. Wittig, J. Appl. Phys. **52**, 4572 (1981).
[27] S. K. Sikka and V. Vijayakumar, Physica B **144**, 23 (1986).
[28] N. Hamaya, Y. Sakamoto, H. Fujihisa, Y. Fujii, K. Takemura, T. Kikegawa, and O. Shimomura, J. Phys. C **5**, L369 (1993).
[29] M. I. McMahon and R. J. Nelmes, Phys. Rev. Lett. **78**, 3884 (1984).
[30] K. Syassen, A. Grzechnik, J. Kohler, and I. Loa, ESRF Annual Report No. HS1132-ID 09, 2000 (unpublished).
[31] R. Patterson, C. K. Saw, and J. Akella, J. Appl. Phys. **95**, 5443 (2004).
[32] M. H. Ben Ghozlen and Y. Mlik, J. Phys. C **16**, 4365 (1983).
[33] H. T. Stokes and D. M. Hatch, Phys. Rev. B **30**, 4962 (1984).
[34] W. A. Grosshans, Y. K. Vohra, and W. B. Holzapfel, Phys. Rev. Lett. **49**, 1572 (1982).
[35] F. Porsch and W. B. Holzapfel, Phys. Rev. B **50**, 16212 (1994).
[36] M. Seipel, F. Porsch, and W. B. Holzapfel, High Press. Res. **15**, 321 (1997).
[37] F. Birch, J. Geophys. Res. **83**, 1257 (1978).
[38] W. A. Grosshans and W. B. Holzapfel, Phys. Rev. B **45**, 5171 (1992).
[39] W. J. Carter, J. N. Fritz, S. P. Marsh, and R. G. McQueen, J. Phys. Chem. Solids **36**, 741 (1975).